

Parallel Adatom Chains on Si(111): A Chemisorption-Induced Surface Reconstruction

G. C. L. Wong,^{1,2} C. A. Lucas,² D. Loretto,² A. P. Payne,³ and P. H. Fuoss³

¹*Department of Physics, University of California, Berkeley, California 94720*

²*Material Sciences Division, Lawrence Berkeley Laboratory, Berkeley, California 94720*

³*AT&T Bell Laboratories, 600 Mountain Avenue, Murray Hill, New Jersey 07974*

(Received 10 May 1994)

Using surface x-ray scattering, we have studied a (3×1) Si(111) reconstruction induced by chemisorption of CaF_2 . This reconstruction consists of a parallel array of zigzag Si adatom chains oriented along $\langle 1\bar{1}0 \rangle$. The orbitals on the Si chain atoms rehybridize into p_x and p_y along the surface to form σ bonds, and parallel sp_z orbitals perpendicular to the surface to give additional π bonding. This basic structure, with no dangling bonds at only $\frac{1}{3}$ monolayer adsorbate coverage, may explain the occurrence of (3×1) reconstructions among a diverse range of Si-adsorbate systems.

PACS numbers: 68.35.Bs

There are three known large scale Si(111) surface reconstructions, the (2×1) π -bonded chain structure native to cleaved surfaces [1], the commonly observed (7×7) dimer-adatom-stacking-fault (DAS) structure [2], and a metastable $(\sqrt{3} \times \sqrt{3})$ - $R30^\circ$ structure [3]. Recent work has shown that reconstructions with a (3×1) symmetry can also be generated on Si(111) by a variety of adsorbates, such as CaF_2 , Ag, and the alkali metals [4–10]. In contrast to the clean surfaces, the precise atomic structures of the adsorbate-induced (3×1) phase is unknown and the subject of considerable debate [7,9,10]. Although a full structural solution was not available, low energy electron diffraction (LEED) measurements reveal strikingly similar intensity-voltage (I - V) curves for the (3×1) phases induced on Si(111) by Li, Na, K, Cs, and Ag, adsorbates with widely differing atomic sizes [6]. This strongly suggests that the observed (3×1) phase is predominately a Si reconstruction common to the different adsorbates.

In this Letter, we determine the atomic structure of a chemisorption-induced, large scale (3×1) Si reconstruction using *in situ* x-ray scattering. CaF_2 is an ionic insulator with an fcc-type structure and lattice constant similar to Si, and has been observed to form a series of ordered reconstructions on Si(111)- 7×7 with increasing submonolayer coverages [5]. The first of these is a (3×1) phase, which forms at coverages from as low as $\sim \frac{1}{10}$ monolayer (ML), to as high as $\sim \frac{1}{3}$ ML [11,12]. We find that the $\text{CaF}_2/\text{Si}(111)$ - (3×1) reconstruction is primarily a Si reconstruction, with a parallel array of zigzag Si adatom chains oriented along $\langle 1\bar{1}0 \rangle$. The basic structural unit, the adatom chain, forms a five-member ring in $\langle 1\bar{1}0 \rangle$ projection. The domain size of the (3×1) phase is comparable to that of the original Si(111)- (7×7) reconstruction on our samples. Moreover, this surface structure, with no dangling bonds at only $\frac{1}{3}$ monolayer adsorbate coverage, may explain the occurrence of (3×1) reconstructions among a diverse range of Si-adsorbate systems.

The experiment was performed at beam line X-16A of the National Synchrotron Light Source (NSLS), with an

ultrahigh vacuum (UHV) system coupled to a five-circle diffractometer [13]. Dipole magnet radiation was focused to a beam size of $\sim 1.0 \text{ mm} \times 1.5 \text{ mm}$ at the sample, and monochromatized to a wavelength of 1.37 \AA . For the in-plane measurements, the incident angle of the x-ray beam to the sample surface was equal to the exit angle, $\beta = 0.7^\circ$, which is well above the Si critical angle. Scattered x rays were collected using a position-sensitive detector held at a constant angle relative to the sample surface, and binned to give an angular resolution of $\sim 0.35^\circ$ along the sample surface normal.

The Si(111) sample used in this experiment (measured miscut of $\sim 0.2^\circ$) was cleaned using the Shiraki method [14], and loaded into the vacuum chamber. After being thoroughly outgassed, the Si sample was heated to 1000°C in order to remove the protective oxide (the sample temperature was monitored using an optical pyrometer); the (7×7) reconstruction of clean Si(111) was obtained upon subsequent cooling. X-ray measurements of representative (7×7) superstructure reflections were consistent with previous results [15]. CaF_2 was evaporated from a Knudsen cell, and deposited onto the Si sample at 700°C . During deposition, the chamber pressure increased from the base value of $\sim 1 \times 10^{-10}$ torr to the 10^{-9} torr range. Apart from the initial growth calibration experiments, all survey scans were done with x rays rather than with LEED, in order to avoid electron beam damage. Although a (3×1) reconstruction could be observed using x rays immediately after deposition, the measured third-order peak intensities became stronger, and the peak widths narrower, after a 2 min anneal at 775°C . The average correlation length obtained from the full width at half maximum (FWHM) of superstructure reflections was $\sim 3000 \text{ \AA}$, comparable to that of the Si (7×7) reconstruction on our samples.

Integrated intensities for each reflection are obtained by fitting Lorentzian line shapes with flat backgrounds to rocking scans about the surface normal. By applying the standard corrections for polarization, Lorentz factor, and variation of active sample area, the absolute square of the

structure factors is obtained. Periodic remeasurements of a (3×1) reflection during the data collection period of ~ 24 h revealed no noticeable sample degradation. A total of 88 superstructure reflections were collected from two of the three rotational domains of the (3×1) reconstruction [16]. The resulting data set is symmetry averaged, leading to a final data set of 13 irreducible structure factors, F_{hk} , indexed using hexagonal surface diffraction notation: $\mathbf{a}_1 = (1/2)[10\bar{1}]_{\text{cubic}}$, $\mathbf{a}_2 = (1/2)[\bar{1}10]_{\text{cubic}}$, $\mathbf{a}_3 = [111]_{\text{cubic}}$. The count rate for the strongest superstructure reflection was ~ 200 counts/sec. In order to give more weight to the stronger reflections, we have used an *ad hoc* estimate of the error $\sigma_s = s_{\text{min}} + s/10$, where s is the intensity of the measured reflection, and s_{min} is the intensity of the weakest reflection [17]. This corresponds to an average error of $\sim 10\%$ in the amplitudes, smaller for the strong reflections, larger for the weak.

The model-independent, 2D Patterson pair-correlation function is calculated from the observed structure factors according to

$$P(x, y) = \sum_{h,k} |F_{hk}|^2 \cos 2\pi(hx + ky).$$

There are three irreducible nonorigin peaks within the (3×1) supercell [Fig. 1(a)]. Vectors from the origin to these peaks correspond to interatomic vectors in the surface structure. Based on this Patterson function, no model consisting of Ca and/or F atoms alone can reproduce the data. With the inclusion of two additional Si atoms, rough agreement between the calculated and observed structure factors can be achieved, if the Ca, F, and Si atoms are arranged as in the single fluorine model [see Fig. 2(a)]. However, attempts to refine this model by using a least-squares fitting routine, and allowing the atoms to relax along the mirror plane directions, failed to fully reproduce the data. The fits are quantified with the reduced χ^2 coefficient [18], and the best fits using the single fluorine model give $\chi^2 \sim 6$. A map of the difference in electron density between the calculated experimental and calculated models, $\Delta\rho(x, y)$, can be made by assuming that the model generated by the Patterson function is close enough to the real structure so that the calculated phases of F_{hk} , α_{hk}^{cal} , are close to the experimental phases [19]:

$$\Delta\rho(x, y) = \sum_{h,k} (|F_{hk}^{\text{exp}}| - |F_{hk}^{\text{cal}}|) \cos[2\pi(hx + ky) - \alpha_{hk}^{\text{cal}}].$$

The difference map reveals two distinct peaks [Fig. 1(b)], which indicate the places where the single fluorine model is deficient in electron density relative to the data. The larger feature is located near a position assigned to a F atom. Two possibilities exist: Either the atom at the position in question has a larger atomic number than that of a F atom, or an additional F atom exists in the structure, at a position that was obscured by the additional inversion symmetry introduced by the Patterson function (see the double fluorine model of Fig. 2). Substitution of Si or Ca atoms for the F atom in the single fluorine model

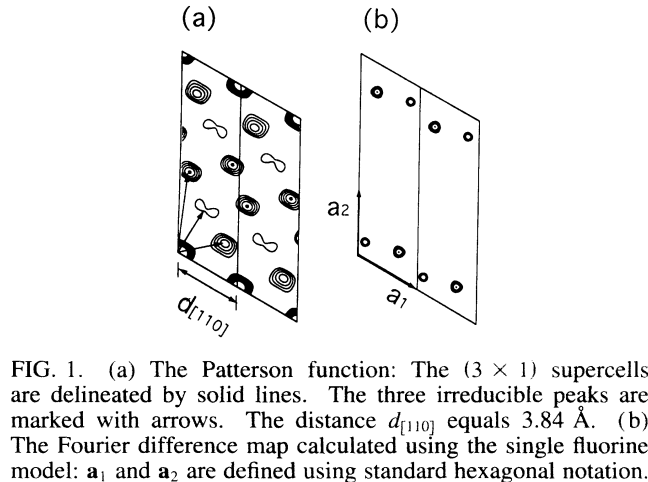


FIG. 1. (a) The Patterson function: The (3×1) supercells are delineated by solid lines. The three irreducible peaks are marked with arrows. The distance $d_{[110]}$ equals 3.84 \AA . (b) The Fourier difference map calculated using the single fluorine model: \mathbf{a}_1 and \mathbf{a}_2 are defined using standard hexagonal notation.

increases χ^2 . Addition of a second F atom, however, dramatically improves the fits. The final model, refined using four relative atomic positions, a Debye-Waller factor, and a scale factor, gives $\chi^2 = 1.34$. A difference map calculated using the new model yields only noise. A comparison between measured and calculated F_{hk} is given in Fig. 3, and shows the excellent agreement.

It is unlikely that the Si chain atoms are registered at threefold sites, such as H_3 and T_4 , since large bond length distortions are necessary for chain formation. Si atoms on atop sites, however, only need to change the bond angle

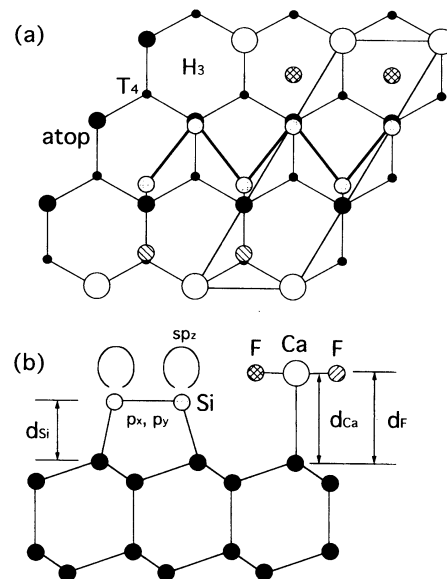


FIG. 2. (a) Top view of the double fluorine model: the single fluorine model is obtained by removal of the double-hatched F atoms. The Si-Si distance on the chains is $2.67 \pm 0.09 \text{ \AA}$. The average Ca-F distance is $2.47 \pm 0.10 \text{ \AA}$ (natural bond length: 2.37 \AA). The fitted value of the Debye-Waller parameter for the adsorbed Ca and F atoms is 0.75 \AA^2 . (b) $\langle 1\bar{1}0 \rangle$ projection of the final model: The fit parameters from the $(1\ 0\ l)$ rod are as follows: $d_{\text{Si}} = 2.0 \pm 0.1 \text{ \AA}$, $d_{\text{Ca}} = 3.0 \pm 0.1 \text{ \AA}$, $d_{\text{F}} = 3.1 \pm 0.1 \text{ \AA}$. Schematic sp_z orbitals are also depicted.

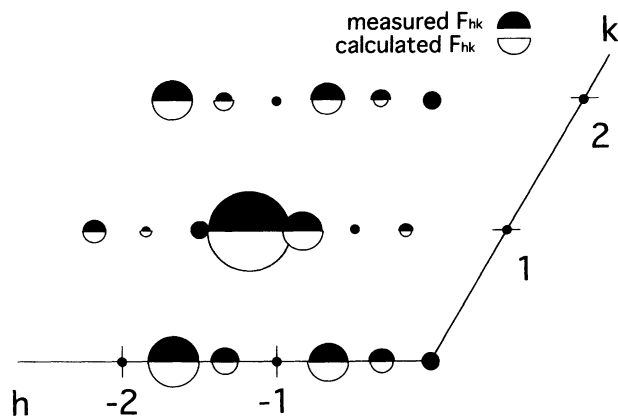


FIG. 3. The measured and calculated (3×1) structure factors F_{hk} are represented by pairs of semicircular sectors. The radii are proportional to the amplitudes; the areas to the intensities. The larger filled circles represent in-plane bulk Bragg reflections and the smaller ones represent the crystal truncation rods. The mirror plane in this domain is coincident with the h axis.

for such coupling [Fig. 2(a)], which is more energetically favorable. Crystal truncation rods are sensitive to the interference between scattering contributions from the bulk and the reconstructed layer, and hence contain information on registry. The measured intensity for the $(1\ 0\ l)$ truncation rod (Fig. 4) confirms the atop assignment ($\chi^2 = 1.26$). The fit to the rod is refined on four atomic z coordinates (two for Si, one for Ca, and one for F), a “Debye-Waller” roughness parameter, and an overall scale factor (see Fig. 4). The fit parameters indicate that the Si chain atoms are arranged symmetrically, at a height of 2.0 ± 0.1 Å above the first layer substrate atoms; this implies that the charge transfer between chain atoms is small and may explain why such chain atoms are not readily seen in soft x-ray photoemission [12]. The intensity profiles of the fractional-order rods are sensitive to the thickness of the reconstructed supercell. We measured several of these rods, all of which are essentially flat. The absence of intensity modulations confirms the two-dimensional nature of the reconstruction.

The measured Ca-Si vertical separation from the $(1\ 0\ l)$ rod is 3.0 ± 0.1 Å, which is consistent with Ca atop registry, since Ca-Si bond lengths in CaSi_2 are 3.03–3.25 Å [20]. Medium energy ion scattering studies have indicated that at a (1×1) coverage, the interface Ca atoms are undercoordinated (CaF) and occupy T_4 sites [21]. We have measured the $(1\ 0\ l)$ rod from a sample with a (1×1) coverage, and confirmed the above arrangement, with interface Ca atoms at T_4 sites, bonded to a single fluorine each, resulting in CaF instead of CaF_2 . This implies that the overcoordinated Ca atop sites observed on the (3×1) phase are metastable, and may be related to incomplete F dissociation.

Other structural models for the (3×1) phase have also been considered. Removal of all the F atoms from the

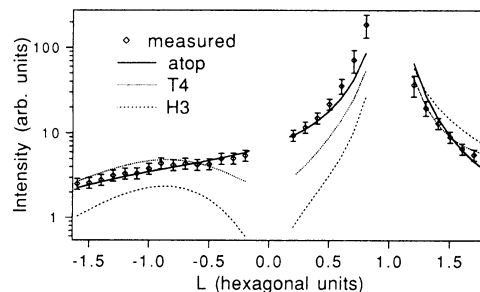


FIG. 4. The measured intensity profile of the $(1\ 0\ l)$ truncation rod, showing the data and the results of least-squares fits using atop, T_4 , and H_3 registries for the origin of the reconstructed supercell, defined at the position occupied by the Ca atom.

model resulted in poor fits to the in-plane data, with $\chi^2 \sim 10$. Permutations of the Si, Ca, and F atoms at the positions given by the Patterson function also gave poor fits, with $\chi^2 \sim 20$. Replacement of the Si atoms on the chain with F or Ca atoms yielded poor agreement as well ($\chi^2 \sim 5$). This is expected, as no F-induced Si $2p$ shift was observed with soft x-ray photoemission [22], and there is no plausible mechanism for negatively charged F ions to couple attractively into chains. The measured interatomic distance on the chain is smaller than reasonable Ca-Ca separations (~ 3.5 – 3.8 Å [23]) by more than 50%. The fact that the Patterson function has only three irreducible peaks argues against more complex (3×1) arrangements, such as the missing row model [6].

The bonding character of the Si atoms along the chains requires careful consideration. A similar scheme with coupled Si chains in $sp_2 + p_z$ hybridization was originally proposed for the (2×1) cleaved surface [24]. The π -bonding scheme proposed for such chains, however, requires large bond angle strains and results in small orbital overlap, as the constituent π -bonding orbitals point away from one another. The measured Si-Si distance on the chains is 2.67 ± 0.09 Å, which is larger than sp_3 (2.35 Å) or sp_2 (2.2 Å) bond lengths. This suggests that the σ bonds along the chains have more p character. If the chain atoms rehybridize from bulklike sp_3 into p_x and p_y along the surface, and parallel sp_z orbitals perpendicular to the surface, then additional π bonding can occur without the need for large bond angle strains, since the constituent orbitals are now parallel as well as more spatially extended [see Fig. 2(b)]. This has two interesting consequences: (1) The p_x and p_y orbitals have charge density minima at the Si atom itself; this can be a potential source of ambiguity in the interpretation of scanning tunneling microscopy (STM) images. (2) This chain arrangement results in a surface with no dangling bonds at only $\frac{1}{3}$ monolayer adsorbate coverage, and suggests the possibility of resonating π bonds and resultant electron delocalization along the chains. Moreover, such quasi-1D chains may be susceptible to a Peierls instability [10,25], a periodic distortion that opens an energy gap at the Fermi

level. This may form the basis of an explanation for the existence of higher order reconstructions like the (3×2) , observed with STM [16], as well as the nonmetallic dispersion of the Ca/Si(111) interface state measured in photoemission [12]. A photoemission measurement of the dispersion along the chain (ΓJ -type) directions would elucidate the electronic structure of this reconstruction, although the multidomain structure of the (3×1) would complicate analysis.

The parallel adatom chain model for the (3×1) reconstruction suggests a possible explanation for the large (3×1) domain sizes, and the large CaF_2 diffusion lengths on this composite surface. CaF_2 deposited at 400°C forms small ($<1000 \text{ \AA}$) islands that punctuate large regions of the (7×7) reconstruction. We have found that by annealing these islands at 700°C , it is possible to form large domains of the (3×1) phase [26]. A surface with no dangling bonds will react only weakly with the strongly bonded CaF_2 molecules ($\Delta H_{\text{dissociation}} = 8.9 \text{ eV/molecule}$ [27]), and may allow the large diffusion lengths necessary for such a transition.

A similar atomic structure has recently been proposed for Ag/Si(111)- (3×1) based on STM and Auger spectroscopy data [10]. The possibility that the parallel adatom chain structure for the (3×1) reconstruction can be induced by such vastly different adsorbates as CaF_2 and Ag is intriguing; it implies that the resultant total energy lowering is largely a consequence of the Si component of the reconstruction. In each instance, the adsorbate saturates rows of dangling bonds, and divides the Si surface into strips 3 unit cells wide. Within these strips the Si reconstructs to eliminate all remaining dangling bonds.

In summary, we have determined the atomic structure of a Si(111)- (3×1) reconstruction induced by chemisorption of CaF_2 . We believe that this low energy configuration with no dangling bonds, using parallel adatom chains as a basic structural unit, can be generalized beyond the present adsorbate system, and may explain the occurrence of (3×1) reconstructions among the diverse range of Si-adsorbate systems.

We would like to thank Oleh Karpenko for his contributions to this work. We are also grateful to Peter Eng for his assistance at X-16A, Chuck Fadley, S. Y. Tong, Frank Lamelas, Frances Ross, J. Denlinger, and E. Rotenberg for helpful discussions, and S. Yalisove for a critical reading of the manuscript. This work was supported by the Director, Office of Basic Energy Sciences, Materials Sciences Division of the U.S. Department of Energy under Contract No. ACO3-76SF00098. NSLS is supported by the Department of Energy under Grant No. DE-AC012-76CH00016.

[1] K. C. Pandey, Phys. Rev. Lett. **47**, 1913 (1981); **49**, 223 (1982).

[2] K. Takayanagi, Y. Tanishiro, S. Takahashi, and M. Takahashi, Surf. Sci. **164**, 367 (1985).

- [3] W. C. Fan, A. Ignatiev, H. Huang, and S. Y. Tong, Phys. Rev. Lett. **62**, 1516 (1989).
- [4] R. J. Wilson and S. Chiang, Phys. Rev. Lett. **58**, 369 (1987).
- [5] C. A. Lucas, G. C. L. Wong, and D. Loretto, Phys. Rev. Lett. **70**, 1826 (1993).
- [6] W. C. Fan and A. Ignatiev, Surf. Sci. **296**, 352 (1993); Phys. Rev. B **41**, 3592 (1990).
- [7] D. Jeon, T. Hashizume, T. Sakurai, and R. F. Willis, Phys. Rev. Lett. **69**, 1419 (1991).
- [8] K. J. Wan, X. F. Lin, and J. Nogami, Phys. Rev. B **46**, 13635 (1992).
- [9] See, for example, Bull. Am. Phys. Soc. **39**, 256, E15.9, E15.10, I15.14 (1994).
- [10] H. H. Weitering, J. Chen, N. J. DiNardo, and E. W. Plummer, Phys. Rev. B **48**, 8119 (1993); See also Bull. Am. Phys. Soc. **39**, 256, E15.8, G'4.2 (1994).
- [11] G. C. L. Wong, C. A. Lucas, and D. Loretto (unpublished); also, J. Denlinger (private communication).
- [12] Marjorie A. Olmstead, R. I. G. Uhrberg, R. D. Bringans, and R. Z. Bachrach, J. Vac. Sci. Technol. B **4**, 1123 (1986).
- [13] P. H. Fuoss and I. K. Robinson, Nucl. Instrum. Methods Phys. Res., Sect. A **222**, 164 (1984); E. Vlieg *et al.*, J. Appl. Cryst. **20**, 330 (1987).
- [14] A. Ishizaka and Y. Shiraki, J. Electrochem. Soc. **133**, 666 (1986).
- [15] I. K. Robinson, J. Vac. Sci. Technol. A **6**, 1966 (1988), and references therein.
- [16] We found that one domain was considerably weaker than the other two, and hence it was not used in the averaging. Such domain behavior is similar to results from Ph. Avouris and R. Wolkow, Appl. Phys. Lett. **55**, 1074 (1990).
- [17] F. J. Lamelas, P. H. Fuoss, D. W. Kisker, G. B. Stephenson, P. Imperatori, and S. Brennan, Phys. Rev. B **49**, 1957 (1994).
- [18] The reduced χ^2 coefficient is normalized by $1/(N - P)$, where N is the number of data points and P is the number of free parameters.
- [19] See, for example, J. Bohr, R. Feidenhans'l, M. Nielsen, M. Toney, R. L. Johnson, and I. K. Robinson, Phys. Rev. Lett. **56**, 2878 (1986).
- [20] J. F. Morar and F. Wittmer, Phys. Rev. B **37**, 2618 (1988).
- [21] R. M. Tromp and M. C. Reuter, Phys. Rev. Lett. **61**, 1756 (1988).
- [22] Work performed by Marjorie A. Olmstead, J. D. Denlinger, Eli Rotenberg, and G. C. L. Wong at Stanford Synchrotron Radiation Laboratory (unpublished).
- [23] E. Clementi, D. L. Raimondi, and W. P. Reinhardt, J. Chem. Phys. **47**, 1300 (1967); see also the Ca-Ca separations in CaSi_2 , CaSi , and Ca_2Si , as listed in O. Bisi *et al.*, Phys. Rev. B **40**, 10194 (1989).
- [24] R. Seiwatz, Surf. Sci. **2**, 437 (1964).
- [25] See, for example, G. Gruner, Rev. Mod. Phys. **60**, 1129 (1988).
- [26] C. A. Lucas, D. Loretto, and G. C. L. Wong, (to be published).
- [27] *Gmelins Handbuch der Anorganischen Chemie, Ca Teil B, Lieferung 2* (Springer-Verlag, Berlin, 1974), 8th ed.